sciendo

LATVIAN JOURNAL OF PHYSICS
AND TECHNICAL SCIENCES
2021, N 1

DOI: 10.2478/lpts-2021-0001

THERMOLUMINESCENCE RESPONSE OF AlN+Y_2O_3 CERAMICS TO SUNLIGHT AND X-RAY IRRADIATION

J. Cipa*, L. Trinkler, B. Berzina

Institute of Solid State Physics, University of Latvia,
8 Kengaraga Str., Riga, LV-1063, LATVIA
*e-mail: janis.cipa@cfi.lu.lv

AlN is a wide band gap material with promising properties for dosimetric applications, especially in UV dosimetry. In the present research, the thermoluminescence method is used in order to better understand sunlight and X-ray irradiation effects on yttria doped AlN ceramics. In general, the TL response is characterised by a broad TL peak with maxima around 400–450 K and a TL emission spectrum with UV (400 nm), Blue (480 nm) and Red (600 nm) bands. Compared to the X-ray irradiation, sunlight irradiation creates a wider TL glow curve peak with a maximum shifted to higher temperatures by 50 K.

Furthermore, in the TL emission spectra of AlN irradiated with sunlight the UV band is suppressed. The reasons of the TL peculiarities under two types of irradiation are discussed. Practical application of AlN ceramics as material for UV light TL dosimetry and, in particular, for sunlight dosimetry is estimated.

Keywords: *AlN, sunlight, thermally stimulated luminesce, UV light dosimetry, X-ray radiation.*

1. INTRODUCTION

Thermally and optically stimulated luminesce can be used to understand defect structure of materials, but in some cases the investigated material can have a combination of desirable dosimetric properties such as high response to irradiation, large linear dynamic dose range, stable signal during storage and others, making it suitable as a dosimetric material. AlN is one of such materials. There are currently commercially available dosimeters such as LiF:Mg,Cu,P (TL) Al_2O_3:C (OSL) and others, which can be used for different applications. Nevertheless, there is a demand for new dosimetric materials in some dosimetry areas, such as OSL neutron dosimetry, 2D dose

mapping, temperature sensing, UV dosimetry and others [1], [2].

UV light dosimetry is important because exposure to solar ultraviolet radiation is considered a risk to public health due to the increase of skin cancer incidence in the world; besides, the work environment with the use of UV light such as welding and water treatment cannot be monitored properly as there is not a lot of choice for dosimetric materials. Some thermoluminescence detectors have been studied as possible UV light dosimeters (LiF:Mg, CaF_2:Dy, CaF_2:Mn, Al_2O_3, LiF:Mg, $CaSO_4$:Dy, CaF_2:TB_4O_7, Vycor glass), but only few of them have found practical application: Al_2O_3:C (TLD-500) and $CaSO_4$:Dy (TLD-900) [3]. They show promising features but also have some certain disadvantages; thus, new dosimetric materials sensitive to UV light are required. In case of AlN, its spectral absorption is similar to that of human skin. Furthermore, it has a high TL response intensity and a large linear dose region. Thus, it might be a perspective UV dosimeter [4]. The main disadvantage of AlN is a high signal fading rate at room temperature, which is not acceptable for dosimetric material. There are multiple ways how to solve this problem, one of them is thermal pre- or post-treatment [5].

To improve dosimetric properties of material, it is critical to understand TL mechanisms and defect structure, which has been thoroughly studied before [4], [6]. The previous studies [7] have shown that AlN ceramics reveals high sensitivity both to ionizing radiation and to UV light; however, each type of radiation provides its own characteristic features of the produced TL signal. In our previous study of luminescence processes induced by UV light irradiation, including TL, it was confirmed that both delocalised and localised electron transitions occur in AlN [8]. Here by delocalised electron transitions we understand those, which take place through the conduction band, while the localised transitions occur directly through tunnel recombination between donor and acceptor centres.

The main efforts of this study are focused on understanding the differences in TL response for AlN+Y_2O_3 irradiated with sunlight and X-rays.

2. EXPERIMENTAL

2.1. Sample Preparation

AlN+Y_2O_3 samples were produced at Riga Technical University by sintering ceramics from mixture of powders. AlN macro powder (20–80 μm, high purity, STREM Chemical Inc) was mixed with Y_2O_3 2 wt% (purity 99.9 %, Fluka) using Fritsh grinding apparatus for 30 min. Though the AlN raw material is nominally pure, it contains traces of Mn impurity revealed in photoluminescence (PL) and TL spectra as an emission band at 600 nm. A graphite press form with diameter of 20 mm was filled with the prepared powder mixture. The press form was placed in a spark plasma sintering apparatus and heated up to 1973 K for 10 min. The obtained AlN +Y_2O_3 ceramics samples with diameter of 20 mm and height of 2 mm were cleaned from admixture of graphite and cut into four pieces for further studies.

The phase composition and crystallite size were determined using an X-ray diffraction (XRD) analysis. Samples of sintered AlN with Y_2O_3 showed characteristic AlN diffraction patterns and contained traces of $Al_5Y_3O_{12}$ compounds. Crystallite

size of the samples was in the range of 56–67 nm depending on sintering temperature, holding time and composition.

2.2. Methods and Equipment

The TL measurements were done with Lexsyg Research TL/OSL reader from Freiberg Instruments. Two types of sample irradiation were used: natural sunlight and X-rays. Sample irradiation with sunlight occurred in summertime when the number of sunny days was the largest.

The Sun emission spectrum on the ground level is shown in Fig. 1 [9]. Its short wavelength part is limited by atmospheric absorption at around 290 nm. In the scope of this study, three types of optical glass filters were used. Their spectral transmission is shown in Fig. 1. Originally, filters are designated by Cyrillic letters; here in the text we give their Latin transcription.

Sample irradiation with X-rays was done by an X-ray source (W anode, anode voltage: 40 kV, anode current: 0.5 mA, irradiation time: up to 60 sec) integrated in the TL reader. To obtain spectra of TL, Andor SR-303i-B spectrometer with DV420A-BU2 CCD (150 lines/mm, 500 nm blaze) camera was coupled to Lexsyg TL/OSL reader with Ultra low-OH Molex optical fiber. While for TL glow curves the integrated Hamamatsu PMT R13456 with spectral range of 185–980 nm was used.

TL was measured at a heating rate of 1 K/s, up to maximum temperature of 700 K where the thermal radiation of the heater was limited by an infrared region and did not interfere with the TL signal. Previous studies have reported an intense afterglow signal for the irradiated AlN ceramics. Thus, after each irradiation a 10-minute delay time was used to decrease the influence of afterglow to < 1 %.

In order to clear up the optically stimulating effect of the visible range of the Sun emission on the stored TL response, the previously sunlight-irradiated AlN+Y_2O_3 sample was exposed to sunlight for 10 minutes through the ZHS16 optical filter, transmitting light with wavelengths longer than 450 nm (see Fig. 1). The obtained TL response was compared with that from the reference sample kept in darkness after irradiation. This method is further designated as sunlight optical stimulation (OS).

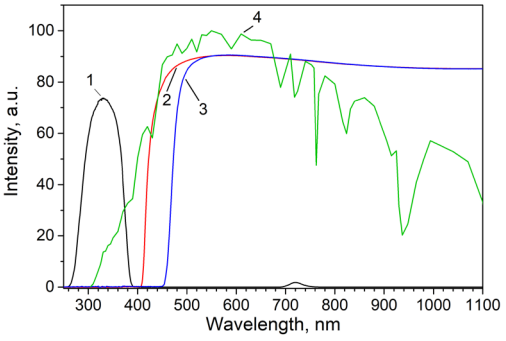

Fig. 1. Transmission spectra of optical glass filters: 1) UFS2, 2) ZHS11, 3) ZHS16 used in this study and 4) the Sun emission spectra on the ground level (redrawn from [9]).

3. RESULTS

3.1. TL Characteristics after Irradiation with Sunlight

To determine the UV light-induced TL properties, we used the Sun as a natural UV light source. We used optical filters to select UV and visible spectral ranges of

the sunlight. It is known that UV light of the Sun emission spectra can excite TL in AlN+Y_2O_3, but also the visible light with wavelengths above 400 nm produces a weak TL signal. Temperature/wavelength contour plots of TL signal from AlN+Y_2O_3 ceramics irradiated with the sunlight without any filters and through UV and yellow filters are displayed in Fig. 2.

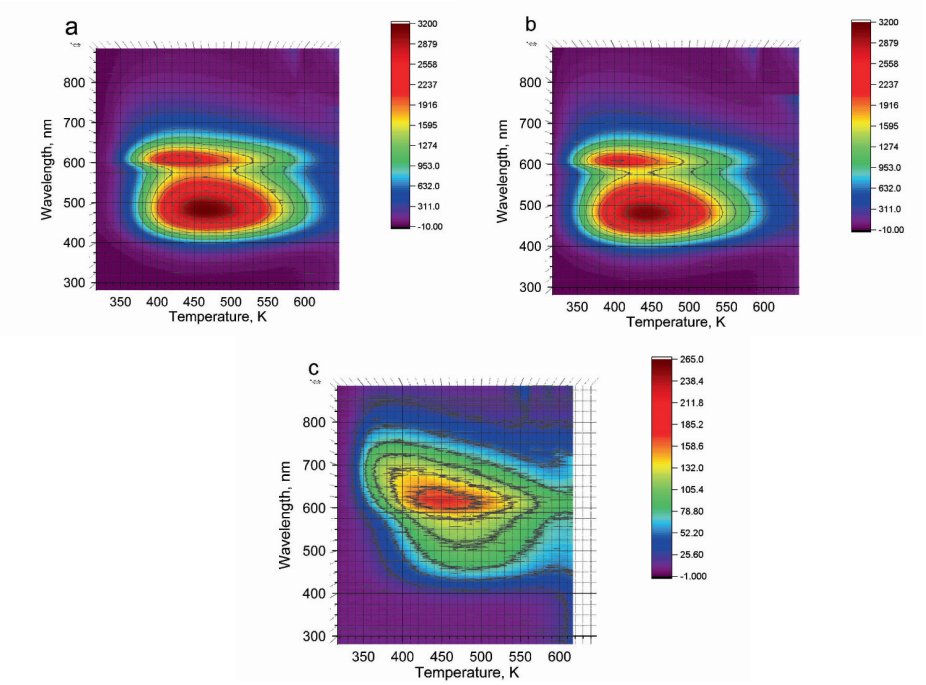

Fig. 2. Contour plots of AlN+Y_2O_3 ceramics irradiated with sunlight: a) without filters; b) through UFS2 filter and c) through ZHS11 filter.

3.1.1. TL Emission after Sunlight Irradiation

Let us compare TL emission spectra of AlN+Y_2O_3 and photoluminescence (PL) emission spectrum. According to the photoluminescence spectra described in our previous papers [10], PL spectrum contains several emission bands: a wide complex band at 400–550 nm, combined with 400 nm and 480 nm emission bands, associated with V_{Al}-O_N and V_{Al}-$2O_N$ centres, respectively, and 600 nm band attributed to Mn defects [4]. Hereafter, we denote these emission bands as UV, Blue and Red bands, accordingly. All these emission bands occur due to radiative recombination processes between donor and accepter centres.

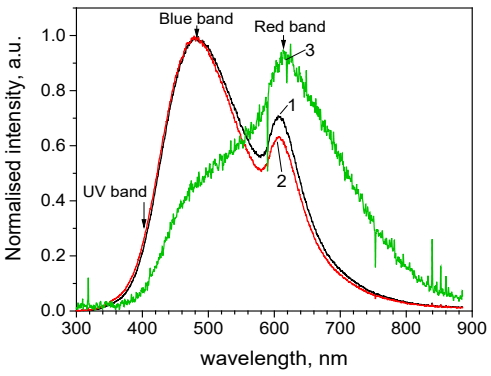

Fig. 3. Normalised TL emission spectra of AlN+Y_2O_3 at 460 K after irradiation with sunlight trough different optical filters: 1) no filter, 2) UFS2 and 3) ZHS11.

The TL emission spectrum contains the same UV, Blue and Red sub-bands as the PL emission spectrum. As seen in Fig. 3, their relative contribution depends on the optical glass filters used during irradiation with sunlight, i.e., on the wavelengths of the irradiation light. Under sunlight irradiation without filters (curve 1), the combined UV+Blue band is dominant over the Red band. Use of the UV filter UFS2 during sunlight irradiation causes a moderate decrease in the intensity of the Red band (curve 2), while ZHS11 filter reduces the total intensity of the TL signal, mainly at the expense of the UV band, so that the Red band becomes dominant (curve 3).

This difference of TL emission spectra under different irradiation conditions can be explained by excitation spectra of AlN individual emission bands [4] and taking into account the concept of the localised electron transitions. In detail, the process of localised electron transitions is described for the UV band of AlN produced by tunnel recombination between V_{Al}-O_N and O_N centres in [8]. As a result, irradiation of the sample with wavelengths, corresponding to absorption of a particular defect centre followed by its excitation and ionisation, causes the predominant appearance of its emission band in the PL and TL emission spectra. It means that excitation with UV light (particularly with sunlight) is selective.

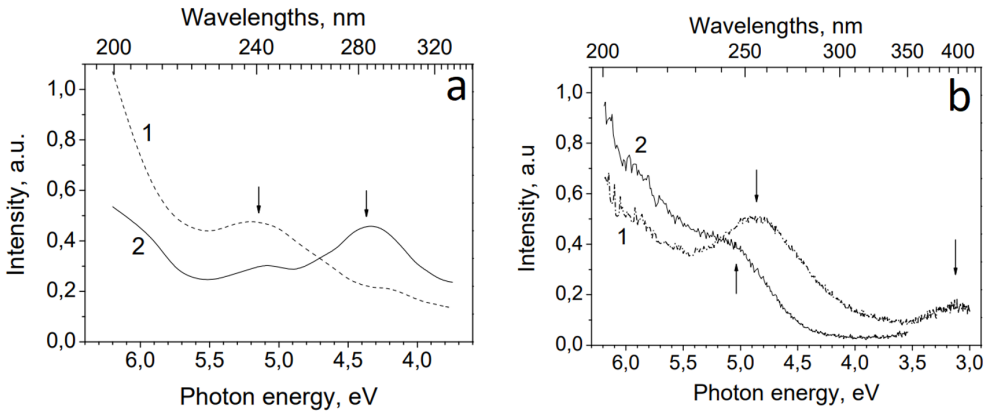

Fig 4. AlN ceramics excitation spectrum at 300 K: a) excitation spectra of 400 nm (1) and 480 nm (2) emission bands and b) excitation spectra of 600 nm band (1) and 400 nm band (2) [4].

Excitation spectrum of AlN ceramics covers a broad spectral range (see Fig. 4). The main excitation bands occur at 250 and 300 nm for the UV emission band, at 290 nm for the Blue emission band and at 260 and 410 nm for the Red emission band. Due to atmospheric absorption, sunlight wavelengths that are shorter than 290 nm do not reach the ground level and, therefore, do not participate in the excitation process. The UV filter UFS 2 cuts off the wavelengths above 390 nm, excluding the 410 nm band from the present excitation spectrum, thus causing reduction of the Red emission band, while still exciting the Blue band. The ZHS11 filter cuts off the wavelengths below 400 nm, eliminating the 290 and 300 nm bands, characteristic of the UV and Blue emission band excitation, from the excitation spectrum, and transmits the 410 nm band, thus decreasing the contribution of the UV (mostly) and Blue bands in favour of the Red band.

3.1.2. Analysis of TL Curves

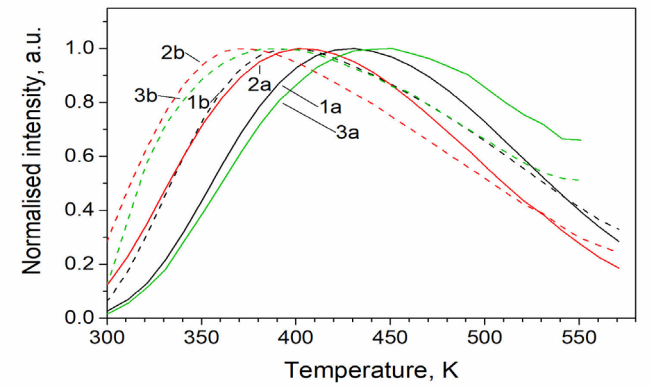

Fig. 5. TL curves after irradiation with sunlight through different optical filters:
1) no filter, 2) UFS2 and 3) ZHS11 for selected
(a) UV+Blue and (b) Red band emission.

Let us compare TL curves obtained after irradiation with sunlight from different spectral regions. Irradiation through the UV filter produces the TL curve peaking at 400 K, while sunlight irradiation without filter causes the TL curve peaking at 420 K. To explain this fact, it should be noted that the full sunlight spectrum causes both generation, predominantly in the UV spectral region, and destruction, in the visible region through the OS process, of the stored TL signal. When sunlight is used for irradiation without filters, both processes occur simultaneously. It is known [4] that the OSL process releases charge carriers from the shallow traps, which would contribute to the low temperature part of the TL curve. As a result, the TL curve obtained under irradiation with the full sunlight emission spectrum loses its low-temperature part and its maximum is shifted to higher temperatures.

Under similar irradiation conditions, the TL curves connected with the Red emission are shifted to lower temperatures compared with the UV+Blue emission (see corresponding curves in Fig. 5). It could be explained by the fact that Mn related trap centres are shallower than the intrinsic O and N related defects, which recombine at lower temperatures.

From our measurements, it is seen that maximum of the TL curves is located around 450 K (see Fig. 2). Yet there is an inconstancy with the results of our previous studies, where the TL curve maximum was found at around 600 K. Possible explanation might be in the different synthesis procedures of ceramic samples as well as different trace element concentration in raw materials. Similar results were reported in [11] where the authors used a synthesis method similar to ours, while slight changes in ceramics production procedure led to occurrence of the TL peak at temperature above 600 K [12], yet for both of these studies materials were obtained from the same material supplying company. Furthermore, even lower temperature maximum was observed in [13] where a different synthesis method was used. This fact indicates the importance of synthesis parameters such as time and temperature, as well as synthesis method and procedure.

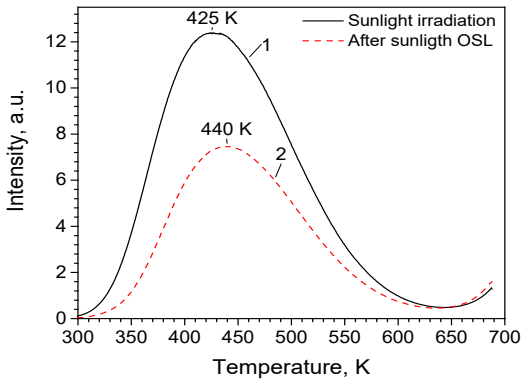

Fig. 6. TL glow curves 1) after irradiation sunlight for 10 min, and 2) after 10 min irradiation + 10 min sunlight OS (irradiation through ZHS16 filter).

As previously mentioned, sunlight both generates and depletes TL signal depending on the selected wavelengths. As for ZHS16 filter sunlight wavelengths shorter than 450 nm are cut off, the TL generating light is absent, but light from the remaining spectra depletes the trap centres. As it can be seen in Fig. 6, after irradiation through ZHS16 filter for the same time as irradiation time, only around half of TL intensity is left.

3.2. TL Characteristics after Irradiation with X-rays

Intensity of the Sun emission and its incident angle depends on a season, time of the day and weather conditions, making it problematic to repeat the accuracy of the experiment. Therefore, X-ray irradiation was chosen as a stable comparative irradiation type. Under X-ray irradiation electrons are transferred from the valence to the conduction band; relaxation of charge carriers is followed by generation of donor and accepter centres, charge carrier capture on luminescent ions and trapping centres. Mutual positioning of the generated luminescent centres and trapping centres is random. Thermal energy supply releases charge carriers from the trap centres; they participate in electron transitions (either delocalized – through the conduction band, or localized due to tunnelling) and radiative recombination. Due to random distribution of the recombination partners generated by the X-ray irradiation, occurrence of luminescence bands in X-ray induced TL emission is non-selective.

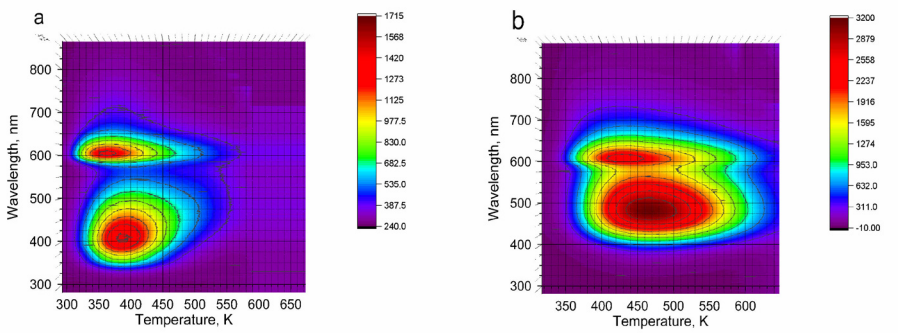

Fig. 7. TL contour plot for AlN + Y_2O_3 irradiated by X-rays for 20 sec (a) and irradiated by sunlight for 10 min (b).

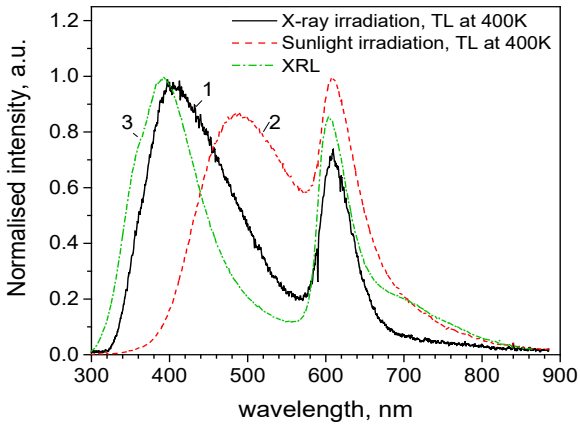

Fig. 8. Normalised TL emission spectra for AlN + Y_2O_3 irradiated 1) by X-rays for 20 sec and 2) by sunlight without filters for 10 min, and 3) X-ray luminescence. All spectra are measured at 400 K.

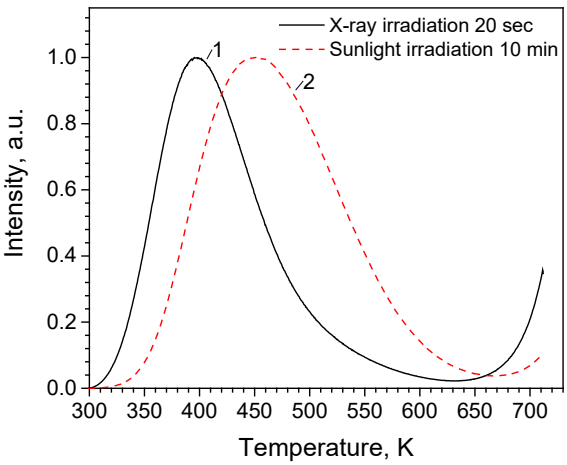

Fig. 9. AlN+Y_2O_3 TL glow curves after 1) X-ray and 2) sunlight irradiation for the integral spectrum.

Let us compare TL properties after irradiation with X-rays and with sunlight without optical filters. Figure 7 shows a noticeable difference between TL contour plots: there is a significant shift to higher temperatures and an essential change in the TL emission spectrum after irradiation with sunlight (Fig.7, b) compared to that with X-rays (Fig.7, a).

In case of AlN+Y_2O_3 ceramics samples the X-ray induced TL emission spectrum (Fig. 8, curve 1) is similar to X-ray luminescence spectrum (see Fig. 8, curve 3). Both spectra contain UV, Blue and Red bands. At the same time, it shows drastic dissimilarity from the sunlight-induced TL emission spectrum, which nearly has no UV band (Fig. 8, curve 2). The spectral difference can be attributed to the non-selective excitation of the UV+Blue bands by X-rays and their selective excitation by sunlight, keeping in mind the short wavelength limit of the sunlight on the ground level, preventing excitation of the UV emission band of AlN +Y_2O_3.

Comparison of the normalised TL

curves is shown in Fig. 9, where X-ray induced thermal curve is peaking at 400 K, while that after sunlight irradiation – at around 450 K. As already mentioned above, one reason for such a difference could be the optical destruction of the stored light sum by visible part of the sunlight spectrum.

Apart from the sunlight-induced OS process, another reason of the TL curve difference after different irradiation types might be related to unintentional heating of the sample during irradiation with sunlight.

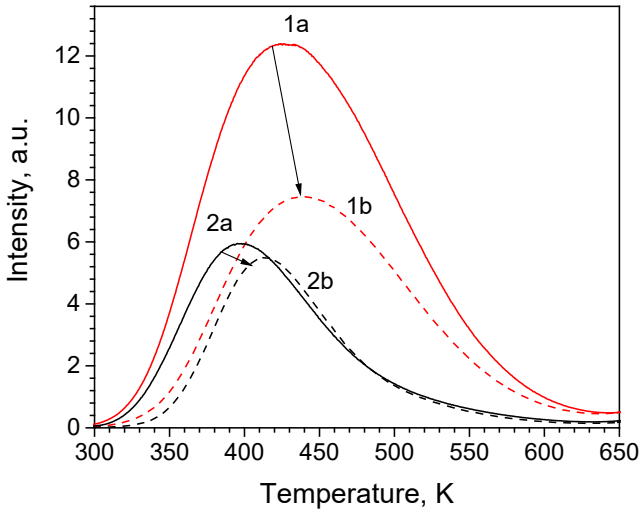

Fig. 10. TL glow curves after irradiation with no-filter sunlight for 10 min (1a) and after direct sunlight irradiation another 10 min irradiation through ZHS 16 filter (1b) and irradiation with X-rays for 20 sec (2a) and Xray irradiation and linear heating up to 330 K in 10 minutes (2b).

To estimate how the sunlight-induced OS and sample heating during irradiation affect the TL curve, a special experiment was implemented (see Fig. 10). It was estimated that during irradiation by sunlight AlN+Y_2O_3 sample might have been heated by approximately 30 K. Thus, further experiments with linear preheating up to 323 K after X-ray irradiation were implemented. The resulting TL curve is shown in Fig. 10, 2b. This TL curve is shifted by 20 K compared to the TL curve without pre-heating.

Secondly, the effect of sunlight OS was investigated. Figure 10 also shows that optical stimulation with wavelengths above 450 nm in 10 minutes reduces TL signal by 40 % and shifts the peak maxima by 15 K. Analysing results of this experiment, it could be concluded that both OS and sample heating during sunlight irradiation reduce the stored TL signal.

In order to control the correctness of the TL response from AlN+Y_2O_3, it is recommended to keep the irradiated material in the darkness and to monitor temperature when samples are irradiated by sunlight.

4. POTENTIAL APPLICATION OF AlN IN UV DOSIMETRY

In this paper, we have investigated the main TL properties of AlN+Y_2O_3 after irradiation with sunlight in comparison with that after X-ray irradiation in order to evalu-

ate its appropriateness as a UV light dosimetry material, and in particular as a material for the sunlight TL detection. In general, AlN ceramics shows rather high sensitivity to the natural sunlight, which is an advantage of the dosimetry material. However, spectral sensitivity of AlN is the highest in the range of 250–270 nm [14], while the Sun emission spectrum is limited by 290–300 nm at the ground level due to absorption by atmospheric oxygen, thus excluding the most favourable region of material sensitivity. Besides, using AlN ceramics for the sunlight dosimetry, one should take into consideration the optical stimulation effect from the light with wavelengths above 450 nm and possible heating of the sample during irradiation, both processes reducing the TL signal. To prevent these effects, optical filters are to be used.

Though AlN could be used for detection of the sunlight dose, its optimal application area lies in the spectral range of 200–300 nm. One of the application areas could be the antibacterial water treatment, where Hg lamps with characteristic emission line at 254 nm are used. This wavelength is particularly favourable for production of the TL signal in AlN ceramics, because it corresponds to the excitation of the UV emission band. AlN ceramics as a dosimetric material could be used to optimise bactericidal reactor configurations and water flow rate [15]. One more possibility could be space applications, where sunlight spectrum is not influenced by atmospheric absorption and AlN could serve as a good dosimeter for astronaut and equipment extravehicular activities [16].

The other effect preventing practical application of AlN for dosimetry is a high fading rate of the stored TL signal. We roughly evaluated a fading rate comparing TL glow curves just after irradiation and 24 h after irradiation. For AlN ceramics, it was determined that 24 h after irradiation the remaining intensity for X-ray irradiated samples was around 50 %, while for sunlight irradiation it was approximately 70%. Taking into account a high fading rate, AlN ceramics could be recommended for quick tests, where it would play an insignificant role.

5. CONCLUSIONS

To summarise, thermoluminescence in $AlN+Y_2O_3$ was investigated after irradiation with sunlight and X-rays. In general, the TL response is characterised with a broad TL peak with maxima around 400–450 K and TL emission spectrum with UV (400 nm), Blue (480 nm) and Red (600 nm) bands. However, there is a significant difference between TL characteristics obtained under irradiation with sunlight and X-rays.

It was found that after sunlight irradiation the obtained TL curve and TL emission spectrum depended on the optical filters used. Specific properties of the TL characteristics are explained by 1) the Sun emission spectrum at the ground level beginning at 290 nm; 2) simultaneous production of the TL signal (by $\lambda < 450$ nm) and its destruction (by $\lambda > 450$ nm) under sunlight irradiation; 3) selective character of production of defect recombination components depending on irradiation light wavelength correspondence to a particular defect absorption; 4) sample heating during irradiation sunlight. The proposed application areas of AlN ceramics as material for UV light TL dosimetry include water treatment and space industry, as well as public sector.

ACKNOWLEDGEMENTS

The present research has been sponsored by the Latvian Council of Science, Grant No. lzp-2018/1-0361. The Institute of Solid State Physics, University of Latvia as the Centre of Excellence has received funding from the European Union's Horizon 2020 Framework Programme H2020-WIDESPREAD-01-2016-2017-Teaming-Phase2 under grant agreement No.73950, project CAMART.[2]

REFERENCES

1. Yukihara, E. G., Milliken, E. D., Oliveira, L. C., Orante-Barrón, V. R., Jacobsohn, L. G., & Blair, M. W. (2013). Systematic Development of New Thermoluminescence and Optically Stimulated Luminescence Materials. *Journal of Luminescence*, *133*, 203–210. https://doi.org/10.1016/j.jlumin.2011.12.018
2. Olko, P. (2010). Advantages and Disadvantages of Luminescence Dosimetry. *Radiation Measurements*, *45* (3–6), 506–511. https://doi.org/10.1016/j.radmeas.2010.01.016
3. Diffey, B. (2020). The Early Days of Personal Solar Ultraviolet Dosimetry. *Atmosphere*, *11* (2). https://doi.org/10.3390/atmos11020125
4. Trinkler, L., & Berzina, B. (2011). Luminescence Properties of AlN Ceramics and Its Potential Application for Solid State Dosimetry. *Advances in Ceramics – Characterization, Raw Materials, Processing, Properties, Degradation and Healing*. https://doi.org/10.5772/18658
5. Burgkhardt, B., Piesch, E., Physk, H., & Nuclear, K. (1978). The Effect of Post-Irradiation Annealing on the Fading Characteristic of Different Thermoluminescent Materials Part II – Optimal Treatment and Recommendations. *Nuclear Instruments and Methods*, *155*, 299–304. https://doi.org/10.1016/0029-554X(78)90219-7
6. Trinkler, L., Berzina, B., Kasjan, D., & Chen, L. C. (2007). Luminescence Properties of AlN Nanostructures Revealed under UV Light Irradiation. *Journal of Physics: Conference Series*, *93* (1). https://doi.org/10.1088/1742-6596/93/1/012040
7. Trinkler, L., Bøtter-Jensen, L., Christensen, P., & Berzina, B. (2001). Stimulated Luminescence of AlN Ceramics Induced by Ultraviolet Radiation. *Radiation Measurements*, *33* (5), 731–735. https://doi.org/10.1016/S1350-4487(01)00093-2
8. Trinkler, L., & Berzina, B. (2014). Localised Transitions in Luminescence of AlN Ceramics. *Radiation Measurements*, *71*, 232–236. https://doi.org/10.1016/j.radmeas.2014.02.016
9. Hulstrom, R., Bird, R., & Riordan, C. (1985). Spectral Solar Irradiance Data Sets for Selected Terrestrial Conditions. *Solar Cells*, *15* (4), 365–391. https://doi.org/10.1016/0379-6787(85)90052-3
10. Trinkler, L., Boøtter-Jensen, L., Berzina, B., Horowitz, Y. S., & Oster, L. (2002). Aluminium Nitrate Ceramics: A Potential UV Dosemeter Material. *Radiation Protection Dosimetry*, *100* (1–4), 313–316. https://doi.org/10.1093/oxfordjournals.rpd.a005876
11. Kojima, K., Okada, G., Fukuda, K., & Yanagida, T. (2016). Influence of SrF2-Doping in AlN Ceramics on Scintillation and Dosimeter Properties. *Radiation Measurements*, *94*, 78–82. https://doi.org/10.1016/j.radmeas.2016.09.008
12. Onoda, Y., Kimura, H., Kato, T., Fukuda, K., Kawaguchi, N., & Yanagida, T. (2019). Thermally Stimulated Luminescence Properties of Eu-Doped AlN Ceramic. *Optik*, *181* (November 2018), 50–56. https://doi.org/10.1016/j.ijleo.2018.11.160

13. Spiridonov, D. M., Weinstein, I. A., Chaikin, D. V., Vokhmintsev, A. S., Afonin, Y. D., & Chukin, A. V. (2019). Spectrally Resolved Thermoluminescence in Electron Irradiated AlN Submicrocrystals. *Radiation Measurements*, *122*, 91–96. https://doi.org/10.1016/j.radmeas.2019.02.001
14. Trinkler, L., & Berzina, B. (2001). Radiation Induced Recombination Processes in AlN Ceramics. *Journal of Physics Condensed Matter*, *13* (40), 8931–8938. https://doi.org/10.1088/0953-8984/13/40/307
15. Li, X., Cai, M., Wang, L., Niu, F., Yang, D., & Zhang, G. (2019). Evaluation Survey of Microbial Disinfection Methods in UV-LED Water Treatment Systems. *Science of the Total Environment, 659*, 1415–1427. https://doi.org/10.1016/j.scitotenv.2018.12.344
16. Dachev, T. P., Tomov, B. T., Matviichuk, Y. N., Dimitrov, P. G., & Bankov, N. G. (2016). High Dose Rates Obtained Outside ISS in June 2015 during SEP Event. *Life Sciences in Space Research, 9*, 84–92. https://doi.org/10.1016/j.lssr.2016.03.004